

Exotic $S = 1$ spin-liquid state with fermionic excitations on the triangular lattice

Maksym Serbyn, T. Senthil, and Patrick A. Lee

Department of Physics, Massachusetts Institute of Technology, Cambridge, Massachusetts 02139, USA

(Received 22 August 2011; revised manuscript received 3 October 2011; published 3 November 2011)

Motivated by recent experiments on the material $\text{Ba}_3\text{NiSb}_2\text{O}_9$, we consider a spin-one quantum antiferromagnet on a triangular lattice with the Heisenberg bilinear and biquadratic exchange interactions and a single-ion anisotropy. Using a fermionic “triplon” representation for spins, we study the phase diagram within mean-field theory. In addition to a fully gapped spin-liquid ground state, we find a state where one gapless triplon mode with a Fermi surface coexists with $d + id$ topological pairing of the other triplons. Despite the existence of a Fermi surface, this ground state has fully gapped bulk spin excitations. Such a state has linear in-temperature specific heat and constant in-plane spin susceptibility, with an unusually high Wilson ratio.

DOI: [10.1103/PhysRevB.84.180403](https://doi.org/10.1103/PhysRevB.84.180403)

PACS number(s): 75.10.Kt, 71.27.+a, 75.10.Jm, 75.30.Kz

The spin liquid (SL) is a long sought exotic state of matter proposed by Anderson,¹ where long-range magnetic order is destroyed by quantum fluctuations at zero temperature. Some materials have been discovered which are promising candidates for the $S = 1/2$ SL state.^{2–6} More recently, possible SL materials with $S = 1$ have been discussed. One example is the insulating spin-1 quantum magnet on a triangular lattice, NiGa_2S_4 , reported by Nakatsuji *et al.*⁷ This material motivated a number of theoretical papers proposing different microscopic realizations of $S = 1$ SL.^{8–11} Recently high-pressure synthesis of the two-dimensional triangular magnet $\text{Ba}_3\text{NiSb}_2\text{O}_9$ (Ref. 12) has produced two phases which possibly realize two- and three-dimensional $S = 1$ SL.

In particular the 6H-B phase, described as a triangular lattice of $S = 1$ Ni^{2+} ions, shows no magnetic ordering down to $T = 350$ mK, well below the Curie-Weiss temperature scale $\theta_{\text{CW}} = -75.5$ K. Such behavior, combined with the frustration of a triangular lattice, suggests the possibility of the SL phase. The spin susceptibility saturates to a constant at low temperatures; specific heat is linear in temperature over a wide range, $T = 0.35\text{--}7$ K, with a high coefficient and Wilson ratio $R_{\text{W}} = 5.6$. Such observations are highly unusual for a magnetic insulator and point to a SL with gapless fermionic excitations. Indeed, to the best of our knowledge, the only other example where such behavior has been seen is the organic $S = 1/2$ SL system.² Quantum fluctuations are less important for $S = 1$, making these data even more striking.

Even within the framework of SL with fermionic excitations, finding a state describing the experiment is a nontrivial problem. For example, a Fermi surface of neutral spin-carrying excitations is strongly coupled to a $U(1)$ gauge field,^{13,14} and the specific heat is expected to behave as $T^{2/3}$. On the other hand, paired SL states in the absence of impurities will typically have $C/T \rightarrow 0$ in the $T \rightarrow 0$ limit. In the present Rapid Communication we propose a candidate SL ground state with a Fermi surface coexisting with fermion pairing which gaps out the gauge field. As a result, this state exhibits the exotic physical properties observed in the experiment. Within the mean field we find our state to be a ground state of a simple Hamiltonian. Our goal is not to find a Hamiltonian which describes the material or to find the ground state of that Hamiltonian. Rather, we are interested in exploring ground states which can explain the specific-heat and susceptibility data and point to further experimental probes of this material.

Our model system consists of quantum $S = 1$ spins forming a triangular lattice. For simplicity, we consider only nearest-neighbor interactions. The general form of the Hamiltonian can be written as

$$H = \sum_{\langle ij \rangle} [J \vec{S}_i \cdot \vec{S}_j + K (\vec{S}_i \cdot \vec{S}_j)^2] + D \sum_i (S_i^z)^2, \quad (1)$$

where we included the Heisenberg exchange interaction with coupling $J > 0$ and the biquadratic exchange with coupling K . In addition, we allow easy-plane or easy-axis type of anisotropy controlled by the parameter D , but we neglect this anisotropy in the couplings J and K since it is presumably small for transition metals. The Hamiltonian (1) has been considered in the literature in the limits when the anisotropy is either zero or dominates over other couplings, or there are longer-range competing exchange couplings. Figure 1 summarizes known results for the ground-state (GS) phase diagram in a schematic way. There are three different phases on the line of zero anisotropy $D = 0$:^{15–18} In the range $K = -0.4J \dots J$, GS is a 120° antiferromagnet (AFM). For larger negative K the system favors collinear ferronematic (FN) order, i.e., nematic order that does not break the lattice translational symmetry. In this state the average spin vanishes $\langle \vec{S} \rangle = 0$, but full spin rotation symmetry is broken down to rotations around an axis specified by the director vector \mathbf{d} (see Refs. 16 and 17 and the discussion below). For positive $K > J$ the ground state is described by aniferromagnetic (AFN) order. In this state the director vectors \mathbf{d}_i on three different sublattices are orthogonal to each other (see Fig. 1), thus breaking the lattice translation symmetry. In the extreme case of easy-plane anisotropy ($D \gg J, |K|$), the GS is a trivial product of states of $|S^z = 0\rangle$ on all sites, corresponding to the trivial single-site FN order. For large but negative D , implying extreme easy-axis anisotropy, only two states with $S^z = \pm 1$ on each site survive. This system can be described by a spin-1/2 XXZ model with all exchange couplings being antiferromagnetic if $2J > K > 0$ or with J^z being frustrating and J^\perp ferromagnetic if $K < 0$. In both cases there is spin-density-wave ordering of the z component of the spin in the GS, supplemented by planar AFN order in the former case and collinear nematic order in the latter case.¹⁹

Physically for $\text{Ba}_3\text{NiSb}_2\text{O}_9$ we may expect the exchange coupling J to be the largest with $J > |K|, |D|$. Both signs of

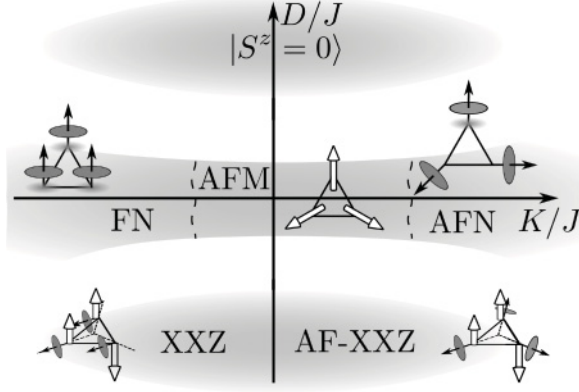


FIG. 1. Schematic representation of the ground state in different limits of the Hamiltonian (1). The white arrows represent average spin; the arrows with disks indicate the director of the nematic order parameter. Details are discussed in the text.

D seems plausible. Likewise, it is not known what sign of the biquadratic exchange K is realized, even though negative K can be obtained from the large U expansion of a certain multiorbital Hubbard model or from coupling to phonons. Therefore, in what follows we study the phase diagram of Hamiltonian (1) for both signs of D and K but will assume $|D|, |K| < J$. Except for very small $|D|$, this is outside of the regions of the known GSs shown in Fig. 1. In order to get access to the [resonating-valence-bond (RVB)-like] state with fermion excitations, we use the fermion representation of the spin.¹⁰ After this we study the resulting phase diagram in the mean-field approximation.

Fermion representation. The spin operator is conveniently represented via a set of three operators called triplons which are labeled by index $\alpha = x, y, z$. In earlier papers^{11,15} these operators were bosons, but here we use fermions¹⁰ written as a vector $\vec{f}_i = (f_{ix}, f_{iy}, f_{iz})^T$,

$$\vec{S}_i = -i \vec{f}_i^\dagger \times \vec{f}_i, \quad \vec{f}_i^\dagger \cdot \vec{f}_i = 1. \quad (2)$$

In terms of S^z eigenstates, we used the following basis to represent the states of $S = 1$, $|x\rangle = i(|1\rangle - |-1\rangle)/\sqrt{2}$, $|y\rangle = (|1\rangle + |-1\rangle)/\sqrt{2}$, $|z\rangle = -i|0\rangle$, since it facilitates the handling of the biquadratic term in the Hamiltonian. Equation (2) also imposes a constraint of single occupation in order to exclude unphysical states from the Hilbert space. In the mean-field theory this constraint will be relaxed to hold only on average. There are two possible choices of constraint for the spin-one system: the particle representation that we used above and the hole representation $\vec{f}_i^\dagger \cdot \vec{f}_i = 2$. In contrast to the case of $S = 1/2$, these are not equivalent. Nevertheless, they can be mapped into each other by a particle-hole transformation plus a change of the sign of hopping. Therefore, we consider only the particle representation but do not restrict hopping to be positive to include the hole representation.²⁰

The chosen spin representation has a remaining $U(1)$ redundancy.^{10,20} One can multiply \vec{f}_i by a phase factor, leaving the spin intact. In addition, in the absence of D there is a spin rotation symmetry, realized by the simultaneous rotation of the vectors \vec{f}_i and $(\vec{f}_i^\dagger)^T$. Nonzero anisotropy D breaks full

spin rotation symmetry to rotation symmetry in the xy plane, supplemented by the reflection of spin along the z axis.

The bilinear term is expressed via fermions as $\vec{S}_i \cdot \vec{S}_j = (\vec{f}_i^\dagger \cdot \vec{f}_j^\dagger)(\vec{f}_i \cdot \vec{f}_j) + \vec{f}_i^\dagger (\vec{f}_i \cdot \vec{f}_j^\dagger) \vec{f}_j$. Using the constraint $\vec{f}_i^\dagger \cdot \vec{f}_i = 1$, the biquadratic term also can be expressed as a product of four fermion operators¹⁵ $(\vec{S}_i \cdot \vec{S}_j)^2 = 1 - (\vec{f}_i^\dagger \cdot \vec{f}_j^\dagger)(\vec{f}_i \cdot \vec{f}_j)$. Adding a Lagrange multiplier to enforce the single occupancy constraint (2) on average, we have

$$H = \sum_{\langle ij \rangle} [J \vec{f}_i^\dagger (\vec{f}_i \cdot \vec{f}_j^\dagger) \vec{f}_j + (J - K)(\vec{f}_i^\dagger \cdot \vec{f}_j^\dagger)(\vec{f}_i \cdot \vec{f}_j) + K] + \sum_i [\mu(1 - \vec{f}_i^\dagger \cdot \vec{f}_i) + D(1 - f_{iz}^\dagger f_{iz})], \quad (3)$$

Mean-field results. Having expressed the Hamiltonian via fermion operators, we study the mean-field phase diagram of our model. To unambiguously decouple quartic fermion terms, we use the Feynman variational principle,^{21,22} which is equivalent to the trial wave-function approach. We define an action based on the Hamiltonian (3) $S = \int_0^\beta d\tau [\sum_i f_{i\alpha}^\dagger (\partial_\tau - \mu) f_{i\alpha} + H]$, as well as the trial quadratic action \tilde{S} , with H replaced by \tilde{H} :

$$\tilde{H} = \sum_{\langle ij \rangle} [\vec{f}_i^\dagger T_{ij} \vec{f}_j + \vec{f}_i^\dagger A_{ij} \vec{f}_j + \text{H.c.}] + \sum_i \vec{f}_i^\dagger t_i \vec{f}_i. \quad (4)$$

The mean-field parameters T_{ij} , A_{ij} , and t_i are determined from the stationary points of the functional $\Psi[\tilde{S}] = \langle S - \tilde{S} \rangle_{\tilde{S}} - \log \tilde{Z}$:

$$\begin{aligned} T_{ij}^{\alpha\beta} &= -J \delta_{\alpha\beta} \langle f_{j\kappa}^\dagger f_{i\kappa} \rangle + (J - K) \langle f_{j\alpha}^\dagger f_{i\beta} \rangle, \\ A_{ij}^{\alpha\beta} &= -J \langle f_{i\beta} f_{j\alpha} \rangle + (J - K) \delta_{\alpha\beta} \langle f_{i\kappa} f_{j\kappa} \rangle, \\ t_i^{\alpha\beta} &= \sum_{\langle ij \rangle} [J \langle f_{j\beta}^\dagger f_{j\alpha} \rangle - (J - K) \langle f_{j\alpha}^\dagger f_{j\beta} \rangle] - D \delta_{\alpha\beta} \delta_{\alpha z}. \end{aligned} \quad (5)$$

For $T = 0$, we get the estimate for the ground-state energy $E_{\text{g.s.}} \leq \tilde{E}_{\text{g.s.}} = \langle H \rangle_{\tilde{S}}$, where

$$\begin{aligned} \tilde{E}_{\text{g.s.}} &= \sum_{\langle ij \rangle} [T_{ij}^{\alpha\beta} \langle f_{i\alpha}^\dagger f_{j\beta} \rangle + A_{ij}^{\alpha\beta} \langle f_{i\alpha}^\dagger f_{j\beta} \rangle] \\ &+ \frac{1}{2} \sum_i [t_i^{\alpha\beta} \langle f_{i\alpha}^\dagger f_{i\beta} \rangle - D \langle f_{iz}^\dagger f_{iz} \rangle + 6K + 2D]. \end{aligned} \quad (6)$$

We search for self-consistent solutions to the mean-field equations that do not break any additional symmetries other than \mathcal{T} reversal. When the full spin rotation symmetry is present, the only possible pairing order parameter is $\Delta_o \sim \langle \vec{f}_i \cdot \vec{f}_j \rangle$. Such pairing preserves full rotational symmetry in spin space, with the resulting state being a spin singlet. We call this pairing an odd channel, since it is possible only with an odd orbital momentum, i.e., p , f -wave pairing. Since in Hamiltonian (1), only *in-plane* rotational symmetry is present for $D \neq 0$, the pairing in the even channel with order parameter $\Delta_e \sim \langle (\vec{f}_i \times \vec{f}_j)_z \rangle = \langle f_{ix} f_{jy} - f_{iy} f_{jx} \rangle$ is allowed. However, the presence of two order parameters simultaneously violates the symmetry with respect to rotations of π around the x or y axis.

Both the aforementioned types of pairing were considered by Liu *et al.*¹⁰ in a similar system, however, without anisotropy but with a competing third-nearest-neighbor J . Their treatment of biquadratic exchange also differs from ours. The result of Ref. 10 was that the pairing in the odd channel always wins. Below, after establishing the mean-field equations for each type of pairing, we identify the region in phase space where even-channel pairing has a lower energy than the odd-channel pairing.

Pairing in an odd channel. We introduce the mean-field parameters χ^α , n^α , and Δ_α^α , $\alpha = x, y, z$, defined as

$$\chi^\alpha = \langle f_{i\alpha}^\dagger f_{i+e_1\alpha} \rangle, \quad n^\alpha = \langle f_{i\alpha}^\dagger f_{i\alpha} \rangle, \quad \Delta_\alpha^\alpha = \langle f_{i\alpha} f_{i+e_1\alpha} \rangle. \quad (7)$$

The vectors $\mathbf{e}_1 = (1, 0)$, $\mathbf{e}_2 = (1/2, \sqrt{3}/2)$, and $\mathbf{e}_3 = \mathbf{e}_2 - \mathbf{e}_1$ specify the link orientation. The hopping is the same on all links, whereas the pairings for the remaining two orientations are $\langle f_{i\alpha} f_{i+e_2\alpha} \rangle = \Delta_\alpha^\alpha e^{i\pi/3}$, $\langle f_{i\alpha} f_{i+e_3\alpha} \rangle = \Delta_\alpha^\alpha e^{2i\pi/3}$, where the pair angular momentum $l = 1, 2, 3$ for $p + ip$, $d + id$, and f -wave pairing, respectively. Spin rotation symmetry in the xy plane requires $\chi^x = \chi^y$, $n^x = n^y$, $\Delta_\alpha^x = \Delta_\alpha^y$. The Hamiltonian in momentum space (modulus nonessential constant terms) can be rewritten as

$$\tilde{H} = \sum_{\mathbf{k}, \alpha} \chi_k^\alpha f_{k\alpha}^\dagger f_{k\alpha} + \Delta_k^\alpha f_{k\alpha}^\dagger f_{-k\alpha} + \Delta_k^{\alpha*} f_{-k\alpha} f_{k\alpha}, \quad (8)$$

with mean-field parameters

$$\chi_k^\alpha = 2\gamma(\mathbf{k})[(J - K)\chi^\alpha - J(\chi^x + \chi^y + \chi^z)] + 6Kn^\alpha - \mu - \delta_{\alpha,z}D, \quad (9)$$

$$\Delta_k^\alpha = \psi(\mathbf{k})[(J - K)(\Delta_\alpha^x + \Delta_\alpha^y + \Delta_\alpha^z) - J\Delta_\alpha^\alpha]. \quad (10)$$

The function $\gamma(\mathbf{k})$ is a sum over nearest neighbors $\gamma(\mathbf{k}) = \cos \mathbf{k} \cdot \mathbf{e}_1 + \cos \mathbf{k} \cdot \mathbf{e}_2 + \cos \mathbf{k} \cdot \mathbf{e}_3$. On the other hand, $\psi(\mathbf{k})$ depends on the type of pairing under consideration. Note that p -wave pairing breaks the lattice rotational symmetry. Therefore, we consider $p + ip$ -wave and f -wave pairings: $\psi^f(\mathbf{k}) = i(\sin \mathbf{k} \cdot \mathbf{e}_1 - \sin \mathbf{k} \cdot \mathbf{e}_2 + \sin \mathbf{k} \cdot \mathbf{e}_3)$, $\psi^{p+ip}(\mathbf{k}) = i(\sin \mathbf{k} \cdot \mathbf{e}_1 + e^{i\pi/3} \sin \mathbf{k} \cdot \mathbf{e}_2 + e^{2i\pi/3} \sin \mathbf{k} \cdot \mathbf{e}_3)$. Equation (8) is solved with the Bogolyubov transformation acting separately on each fermion species. This results in the spectrum $E_k^\alpha = \sqrt{(\chi_k^\alpha/2)^2 + |\Delta_k^\alpha|^2}$, and mean-field equations

$$\chi^\alpha = \frac{1}{N} \sum_{\mathbf{k}} \frac{1}{6} \gamma(\mathbf{k}) \left[1 - \frac{\chi_k^\alpha}{2E_k^\alpha} \right], \quad (11a)$$

$$\Delta_\alpha^\alpha = \frac{1}{N} \sum_{\mathbf{k}} \frac{1}{3} \psi^*(\mathbf{k}) \frac{\Delta_k^\alpha}{2E_k^\alpha}, \quad (11b)$$

$$n^\alpha = \frac{1}{N} \sum_{\mathbf{k}} \frac{1}{2} \left[1 - \frac{\chi_k^\alpha}{2E_k^\alpha} \right], \quad (11c)$$

supplemented by the constraint equation $\langle \vec{f}_i^\dagger \cdot \vec{f}_i \rangle = 1$.

Pairing in an even channel. Hoppings are defined as in (7), whereas pairing is $\Delta_e^{xy} = 1/2 \langle f_{ix} f_{i+e_1y} - f_{iy} f_{i+e_1x} \rangle$. The Hamiltonian is

$$\tilde{H} = \sum_{\mathbf{k}, \alpha} \chi_k^\alpha f_{k\alpha}^\dagger f_{k\alpha} + \Delta_k^{xy} f_{kx}^\dagger f_{-ky} + \Delta_k^{xy*} f_{-ky} f_{kx},$$

with χ_k^α given by Eq. (9), and $\Delta_k^{xy} = 2J\psi(\mathbf{k})\Delta_e^{xy}$. Note, that the f_z band is unpaired and retains its Fermi surface.

We consider s -wave and $d + id$ -wave pairings (the d wave violates lattice symmetry and higher orbital momentum pairing requires inclusion of further neighbors). For the case of s -wave pairing, the function $\psi^s(\mathbf{k}) = \gamma(\mathbf{k})$. For $d + id$ -wave pairing we have $\psi^{did}(\mathbf{k}) = \cos \mathbf{k} \cdot \mathbf{e}_1 + e^{2i\pi/3} \cos \mathbf{k} \cdot \mathbf{e}_2 + e^{-2i\pi/3} \cos \mathbf{k} \cdot \mathbf{e}_3$. The Bogolyubov spectrum is $E_k^x = E_k^y = \sqrt{(\chi_k^{x,y})^2 + |\Delta_k^{xy}|^2}$, $E_k^z = \chi_k^z$. Self-consistent mean-field equations for the x and y components are given by Eq. (11) with the new expressions for the spectrum and gap functions. For the z component we have

$$\chi^z = \frac{1}{N} \sum_{\mathbf{k}} \frac{1}{3} \gamma(\mathbf{k}) n_F(\chi_k^z), \quad n^z = \frac{1}{N} \sum_{\mathbf{k}} n_F(\chi_k^z).$$

Our mean-field approach automatically includes on-site FN order. The on-site nematic order is described by the order parameter tensor $Q^{\alpha\beta} = 1/2 \langle \vec{S}^\alpha \vec{S}^\beta + \vec{S}^\beta \vec{S}^\alpha \rangle - 2/3 \delta^{\alpha\beta}$. For a single site with $S = 1$ all states with zero average spin $\langle \vec{S} \rangle = 0$ can be characterized by the unit director vector \mathbf{d} ,¹⁶ in the basis defined earlier, $|\mathbf{d}\rangle = d_x|x\rangle + d_y|y\rangle + d_z|z\rangle$. For this state $Q^{\alpha\beta}$ is expressed via \mathbf{d} as $Q^{\alpha\beta} = 1/3 \delta_{\alpha\beta} - d_\alpha d_\beta$. For example, $\mathbf{d} \parallel \hat{z}$ corresponds to the state $|S^z = 0\rangle$, and the nematic order is diagonal, $Q^{\alpha\beta} = \text{diag}(1/3, 1/3, -2/3)$. In our model we also have states with vanishing spin order and diagonal on-site nematic order. However, since our GS is RVB like with long-range entanglement, $Q^{\alpha\beta}$ cannot be described by the above simple form. We have to introduce the magnitude q , $Q^{\alpha\beta} = q(1/3 \delta_{\alpha\beta} - d_\alpha d_\beta)$. Calculating the nematic order parameter tensor in our model, we have $Q_i^{\alpha\beta} = \delta_{\alpha\beta} [1/3 - n^\alpha]$, where n^α is the average occupation of corresponding fermion. Since $n^x = n^y$, we have nematic order with $\mathbf{d} \parallel \hat{z}$, with a magnitude given by $q = n^z - n^x$, varying from 1 for $n^z = 1$ (state $|S^z = 0\rangle$) to $-1/2$ for $n^z = 0$. Nonzero anisotropy $D \neq 0$ causes n^α to be different from $1/3$, and therefore directly couples to FN order along the z axis.

Having studied the energies of all the aforementioned states using Eq. (6), we found that the main competition is between states with $p + ip$ and $d + id$ -wave pairings, with all other states being higher in energy. As one increases K , the effective coupling for the odd-channel pairing decreases, whereas for even pairing it remains the same. Finally, for $K \approx 0.45J$, singlet pairing wins. The resulting phase diagram is shown in Fig. 2. The boundary between the two states appears to be weakly dependent on D .

Physical properties of the $d + id$ state. The $d + id$ state breaks the time-reversal symmetry. The chiral order parameter associated with this broken symmetry $\langle \vec{S}_i \cdot (\vec{S}_{i+e_1} \times \vec{S}_{i+e_2}) \rangle \propto \chi^z |\Delta_e^{xy}|^2$ is proportional to the magnitude of the pairing gap squared. In addition, pairing with $d + id$ gap symmetry in two dimensions is topological,²³ resulting in the existence of a pair of zero-energy edge modes at the boundaries. The physics of these modes will be discussed elsewhere.

The combination of gapless excitations with topological pairing gives rise to a number of unusual physical properties that may explain the results of the recent experiment.¹² Due to ungapped f_z excitations, the specific heat depends linearly on temperature near $T = 0$, $C = \pi^2 k_B^2 v_z T/3$, where v_z is the density of states of f_{iz} at the Fermi surface. Due to the Higgs mechanism, the gauge field is massive and does not

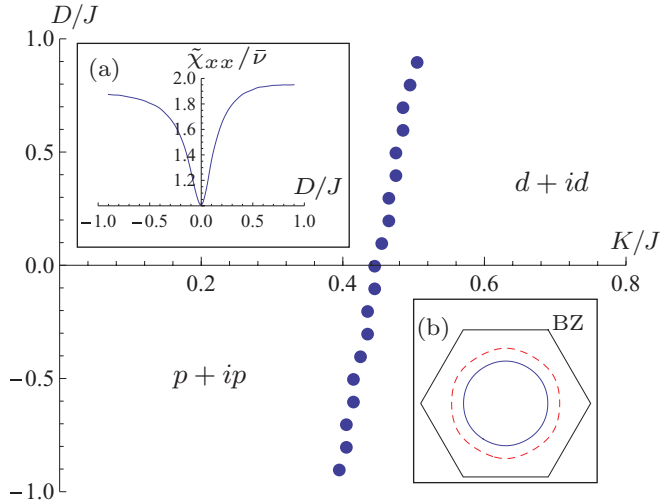


FIG. 2. (Color online) The phase boundary between SL GSs with $p + ip$ and $d + id$ pairing. (a) The spin susceptibility $\tilde{\chi}_{xx}$ in the $d + id$ phase as a function of D/J for $K/J = 0.55$. The susceptibility is normalized by the average density of states $\bar{\nu} = (\nu_x + \nu_z)/2$, where ν_x is calculated without the gap. (b) Gapped (dashed red line) and ungapped (solid blue line) Fermi surfaces of x, y , and z fermions for $K/J = 0.55, D/J = 0.8$.

modify the linear in T behavior of the specific heat. The spin susceptibility exhibits more exotic behavior: Due to the pairing of x and y fermions, the zz component $\chi_{zz} = 0$. On the other hand, χ_{xx} is finite and depends on the anisotropy D . For D smaller than the gap, $\tilde{\chi}_{xx} = \chi_{xx}/(\mu_B g)^2 \approx \nu_z$, and approaches a factor-of-2 larger value $\tilde{\chi}_{xx} \approx 2\nu_z$, when D is much larger than the gap. This difference by a factor of 2 is approximate,

and is valid in the limit of constant gap and density of states. The behavior of $\tilde{\chi}_{xx}$ is shown in Fig. 2(a). We calculate the Wilson ratio, defined as $R_W = (4\pi^2 k_B^2)/(3g^2 \mu_B^2)(\tilde{\chi} T)/C$, and obtain $R_W = 8/3 \approx 2.66$ for the case of small anisotropy, and $R_W \rightarrow 16/3 \approx 5.33$ for large anisotropy. Note that we take the average susceptibility $\tilde{\chi} = 2/3\chi_{xx}$ to account for the polycrystalline nature of the sample. The latter value gives surprisingly good agreement with the Wilson ratio observed experimentally, $R_W \approx 5.63$. We also calculated the imaginary part of the spin susceptibility. Since two out of three fermions are gapped, $\text{Im}\chi_{\alpha\alpha}(\omega, \mathbf{q})$ vanishes for temperatures and frequencies smaller than the gap for all α . This implies that the NMR relaxation $1/(T_1 T)$ is exponentially small for temperatures below the pairing scale. These results tell us that the Fermi surface associated with f_z [see Fig. 2(b)] should be viewed very differently than the spinon Fermi surface in the $S = 1/2$ SL, which carries spin-1/2 quantum numbers and leads to gapless spin-1 excitations. In our case $S^z = 1$ excitations are gapped even though the static spin susceptibility $\chi_{xx}, \chi_{yy} \neq 0$ and the specific heat has a linear T dependence.

Finally, we discuss experiments that could confirm the proposed ground state. Measurement of the spin susceptibility for single-crystal or oriented powder samples is of great interest in order to test our prediction of strong anisotropy. We also predict an exponentially activated behavior for $1/(T_1 T)$ which may be surprising in view of the linear T behavior of the specific heat.

We thank Luis Balicas for bringing Ref. 12 to our attention. We acknowledge useful discussions with Samuel Bieri. T.S. is supported by Grant No. NSF-DMR 6922955. P.A.L. is supported by Grant No. NSF-DMR 1104498.

¹P. W. Anderson, *Mater. Res. Bull.* **8**, 153 (1973); *Science* **235**, 1196 (1987).

²P. A. Lee, *Science* **321**, 1306 (2008).

³Y. Shimizu, K. Miyagawa, K. Kanoda, M. Maesato, and G. Saito, *Phys. Rev. Lett.* **91**, 107001 (2003).

⁴Y. Satoshi, N. Yasuhiro, O. Masaharu, O. Yugo, N. Hiroyuki, S. Yasuhiro, M. Kazuya, and K. Kazushi, *Nat. Phys.* **4**, 459 (2008).

⁵J. S. Helton, K. Matan, M. P. Shores, E. A. Nytko, B. M. Bartlett, Y. Yoshida, Y. Takano, A. Suslov, Y. Qiu, J.-H. Chung, D. G. Nocera, and Y. S. Lee, *Phys. Rev. Lett.* **98**, 107204 (2007).

⁶Y. Okamoto, M. Nohara, H. Aruga-Katori, and H. Takagi, *Phys. Rev. Lett.* **99**, 137207 (2007).

⁷S. Nakatsuji, Y. Nambu, H. Tonomura, O. Sakai, S. Jonas, C. Broholm, H. Tsunetsugu, Y. Qiu, and Y. Maeno, *Science* **309**, 1697 (2005).

⁸S. Bhattacharjee, V. B. Shenoy, and T. Senthil, *Phys. Rev. B* **74**, 092406 (2006).

⁹H. Tsunetsugu and M. Arikawa, *J. Phys. Soc. Jpn.* **75**, 083701 (2006).

¹⁰Z.-X. Liu, Y. Zhou, and T.-K. Ng, *Phys. Rev. B* **81**, 224417 (2010); **82**, 144422 (2010).

¹¹T. Grover and T. Senthil, *Phys. Rev. Lett.* **107**, 077203 (2011).

¹²J. G. Cheng, G. Li, L. Balicas, J. S. Zhou, J. B. Goodenough, and H. D. Zhou, (2011), e-print arXiv:1108.2897.

¹³O. I. Motrunich, *Phys. Rev. B* **72**, 045105 (2005).

¹⁴S.-S. Lee and P. A. Lee, *Phys. Rev. Lett.* **95**, 036403 (2005).

¹⁵N. Papanicolaou, *Nucl. Phys. B* **305**, 367 (1988).

¹⁶A. Läuchli, F. Mila, and K. Penc, *Phys. Rev. Lett.* **97**, 087205 (2006).

¹⁷T. A. Tóth, Ph.D. thesis, EPFL, 2011.

¹⁸P. Li, G.-M. Zhang, and S.-Q. Shen, *Phys. Rev. B* **75**, 104420 (2007).

¹⁹K. Damle and T. Senthil, *Phys. Rev. Lett.* **97**, 067202 (2006).

²⁰This is different from Ref. 10, where authors use a combination of particle and hole constraints in order to preserve particle-hole symmetry. Our treatment violates particle-hole symmetry from the very beginning.

²¹R. P. Feynman, *Statistical Mechanics* (Addison-Wesley, Reading, MA, 1972).

²²J. Brinckmann and P. A. Lee, *Phys. Rev. B* **65**, 014502 (2001).

²³T. Senthil, J. B. Marston, and M. P. A. Fisher, *Phys. Rev. B* **60**, 4245 (1999).